Received: 7 December 2021 | Accepted: 2 February 2022

DOI: 10.1111/bpa.13056

Brain Pathology

RESEARCH ARTICLE

Glial activation in prion diseases is selectively triggered by neuronal PrP^{Sc}

Asvin K. K. Lakkaraju[1] | Silvia Sorce[1] | Assunta Senatore[1] | Mario Nuvolone[1,2,3] | Jingjing Guo[1] | Petra Schwarz[1] | Rita Moos[1] | Pawel Pelczar[4] | Adriano Aguzzi[1]

[1]Institute of Neuropathology, University Hospital of Zurich, Zurich, Switzerland

[2]Amyloidosis Research and Treatment Center, Foundation Scientific Institute Policlinico San Matteo, Pavia, Italy

[3]Department of Molecular Medicine, University of Pavia, Pavia, Italy

[4]Center for Transgenic Models, University of Basel, Basel, Switzerland

Correspondence
Adriano Aguzzi, Institute of Neuropathology, University Hospital of Zürich, Schmelzbergstrasse 12, Zürich 8091, Switzerland.
Email: adriano.aguzzi@usz.ch

Funding information
Stiftung Synapsis - Alzheimer Forschung Schweiz AFS; SystemsX.ch; Schweizerischer Nationalfonds zur Förderung der Wissenschaftlichen Forschung; H2020 European Research Council

Abstract

Although prion infections cause cognitive impairment and neuronal death, transcriptional and translational profiling shows progressive derangement within glia but surprisingly little changes within neurons. Here we expressed PrP^{C} selectively in neurons and astrocytes of mice. After prion infection, both astrocyte and neuron-restricted PrP^{C} expression led to copious brain accumulation of PrP^{Sc}. As expected, neuron-restricted expression was associated with typical prion disease. However, mice with astrocyte-restricted PrP^{C} expression experienced a normal life span, did not develop clinical disease, and did not show astro- or microgliosis. Besides confirming that PrP^{Sc} is innocuous to PrP^{C}-deficient neurons, these results show that astrocyte-born PrP^{Sc} does not activate the extreme neuroinflammation that accompanies the onset of prion disease and precedes any molecular changes of neurons. This points to a non-autonomous mechanism by which prion-infected neurons instruct astrocytes and microglia to acquire a specific cellular state that, in turn, drives neural dysfunction.

KEYWORDS
astrocytes, neurons, prions, scrapie

1 | INTRODUCTION

Prion diseases are characterized by a long, largely asymptomatic incubation period. Once clinical signs and symptoms arise, the disease typically progresses very rapidly. Prion-infected brains contain PrP^{Sc}, an aggregated and misfolded isoform of the cellular prion protein (PrP^{C}) [1]. PrP^{Sc} seeds the nucleation of prions by recruiting PrP^{C}; accordingly, ablation of PrP^{C} abrogates prion propagation [2] and toxicity [3, 4].

The clinical manifestation of prion diseases, both in humans and in animal models, consists of progressive neurological signs including deterioration of cortical functions. The anatomical correlates of the disease are spongiosis (a highly characteristic form of extensive neuronal vacuolation), activation and proliferation of microglia, and astrogliosis. The cortex of patients with terminal prion diseases can show an almost total depletion of neurons [5, 6], which suggests that neurons may be the primary target of the disease. But

Asvin K. K. Lakkaraju, Silvia Sorce, and Assunta Senatore contributed equally to this work.

what is the connection between prion replication and neuronal demise? In a neurografting paradigm, *Prnp*-ablated neurons survive long-term exposure to prions [4], implying that resident PrP^C is necessary for the development of damage. Also, quenching neuronal PrP^C expression was found to delay prion disease [7], adding to the evidence that neuronal PrP^C is required for neurotoxicity.

However, recent molecular studies are painting a starkly different picture. Transcriptomic analysis performed in prion-infected mice over the course of disease has revealed dramatic aberrations of glia-enriched genes coinciding with the onset of clinical signs, whereas neuronal changes were less pronounced and were only detected at the terminal stage of the disease [8]. Similarly, a quantitative analysis of mRNA translation during the course of prion diseases has found that almost all changes during the progression of prion disease occur in non-neuronal cells, except very late in disease [9]. These findings suggest that it is the glia which experiences initial dysfunction, whereas the neuronal demise is a consequence thereof.

Here we have tested the above hypothesis by systematically investigating the impact of cell type-specific PrP^C in disease. We generated transgenic mice line expressing a conditionally expressed PrP transgene, and mated them with mice expressing the Cre recombinase driven by cell type-specific promoters. The resulting mice expressed PrP^C in a cell type-specific manner. We found that neuron-restricted PrP^C sufficed to induce neurodegeneration upon prion infection. Conversely, mice with astrocyte-restricted PrP^C expression did not experience clinical signs of scrapie after prion infection. However, we found that these mice had conspicuous PrP^{Sc} accumulation.

2 | MATERIAL AND METHODS

2.1 | Mice

Animal welfare and experimental procedure on the mice were performed according to the "Swiss Ethical Principles and Guidelines for Experiments on Animals" and approved by the Veterinary office of the Canton of Zurich (permit 90/2013). All efforts were made to minimize the suffering and reduce the number of animals used for the experiments. Mice were bred and housed in special hygienic grade facilities and housed in small groups (max 5 per cage) under a 12 h light/12 h dark cycle with sterilized food (Kilba No.3431, Provimi Kilba Kaiseraugst, Switzerland) and water ad libitum. Prion inoculated mice were regularly monitored according to the standard operating procedures approved by the Veterinary office and mice were humanely sacrificed once the termination criteria were reached.

2.1.1 | Generation of CAG-CAT-PrP transgenic mice

For the generation of mice carrying a *loxP*-flanked stop cassette followed by the mouse *Prnp* coding sequence under the CAG promoter, we used the pCAG–*lox*P–CAT–*lox*P vector (kind gift of Dr. Kimi Araki, Kumamoto University, Japan), where CAG is the CMV immediate early enhancer-chicken β-actin hybrid promoter and CAT the chloramphenicol acetyl transferase gene [10]. Cloning by T4 DNA ligase (New England Biolaboratories, Ipswich, MA, United States) was performed after *Eco*RV (New England Biolaboratories, Ipswich, MA, United States) digestion of both the PCR-amplified *Prnp* cDNA and the pCAG–*lox*P–CAT–*lox*P vector. The *Kpn*I-*Sac*I (New England Biolaboratories, Ipswich, MA, United States) linearized CAG-CAT-*Prnp* transgene was purified and microinjected at the transgenic facility of the University Hospital Zurich into one cell-stage fertilized embryos from $Prnp^{ZH1/ZH1}$ mice. Transgenic founders were identified by PCR using the following primers: Forward: AAC GCC AAT AGG GAC TTT CC; Reverse: ATG GGG AGA GTG AAG CAG AA (actin primers used as internal control for PCR: fwd -TGT TAC CAA CTG GGA CGA CA; rev-GAC ATG CAA GGA GTG CAA GA). Following assessment of germline transmission and establishment of the colonies, the only expresser line (Line 211) was selected based on the levels of CAT expression which were determined in brain tissue homogenates of 2-month-old CAG-CAT-*Prnp* mice using the CAT ELISA kit (Roche, Basel, Switzerland) according to the manufacturer's instructions. Selected line was backcrossed into C57BL6/J background and $Prnp^{ZH3/ZH3}$ for nine generations.

To generate mice expressing Cre recombinase under the control of cell type-specific promoters in ZH3 background: Synapsin1 Cre (B6.Cg-Tg(Syn1-Cre)671Jxm/J(#003966)) and GFAP Cre mice (B6.Cg-Tg(Gfap-Cre)77.6Mvs/2J(#024098)) were bred with ZH3. Cell type-specific Cre expressors in ZH3 background were then crossed with Line 211 to generate mice lines expressing PrP^C exclusively in a subset of neurons (Syn^{Cre};loxPrP) and astrocytes ($GFAP^{Cre}$;loxPrP). Other mice lines used in the current study are: C57BL6/6J and tga20 mice (B6.Cg-Tg(*Prnp*)a20Cwe).

2.1.2 | Prion inoculations

RML6 brain homogenates were prepared from the brains of terminally sick CD1 mice infected with RML6 prions. Brain homogenates were prepared in PBS (+5%BSA). For control inoculations, brain homogenates from healthy CD1 mice were used and they are referred to as noninfectious brain homogenate (NBH). Thirty microliters of RML6 (dose corresponding to 3×10^5 LD_{50}) or NBH lysate was injected intracerebrally into

6- 8-week-old mice. Scrapie was diagnosed according to clinical criteria (ataxia, kyphosis, priapism, and hind leg paresis). Mice were sacrificed on the day of onset of terminal clinical signs of scrapie and NBH inoculated mice were sacrificed approximately at the same time. In case of mice that did not manifest prion disease, they were sacrificed approximately after 550–630 days post inoculations.

2.2 | RNA sequencing and data analysis

RNA extraction from cerebella of mice was performed as described previously [8]. Data analysis and visualizations were performed using Sushi data analysis framework provided by Functional genomics center Zurich (FGCZ) from University of Zurich. Quality control and data analysis were performed as described previously [11]. Differential gene expression was performed using Edge R (version 3.0) [12] and any gene with $Log_2FC > 0.5$ and p-value < 0.05 was considered to be differentially expressed. Data intersection with genes dysregulated during the course of prion infection was performed using Multiple list comparator from www.molbiotools.com.

2.3 | Cerebellar organotypic cultured slices (COCS)

About 350-μm-thick COCS were prepared from 9- to 12-day-old mice pups as described previously [13]. COCS cultures were maintained in a standard incubator (37°C, 5% CO2, 95% humidity) and the medium was replenished three times per week.

2.3.1 | Prion inoculations of COCS

Freshly prepared COCS were inoculated with Rocky mountain laboratory strain 6 prions (RML6) or as a control with either noninfectious brain homogenate (NBH) as described previously. Slices were maintained for a further 56 days followed by fixation with 4% paraformaldehyde and staining with NeuN (to label cerebellar granule neurons), calbindin (to label Purkinjee cells), and DAPI (to label nuclei). Slices were imaged at 4x magnification on a fluorescence microscope (BX-61, Olympus). NeuN and calbindin morphometry was analyzed using analySISvc5.0 software and neurotoxicity was defined as significant loss of NeuN or calbindin-positive neuronal layer loss over NBH treatment.

2.3.2 | POM1 treatment of COCS

Toxicity in COCS was induced by treatment with anti-PrP^C antibody (POM1) targeting the globular domain of the protein as described previously [14]. COCS were treated with either POM1 (67nM) or as control with IgG for 10 days after a 14-day recovery period of initial gliosis due to tissue preparation. COCS were fixed, imaged, and analyzed as described for the prion inoculated slices. Antibody treatment was randomly assigned to individual wells.

2.4 | Western blots

Mice brains (RML6 and NBH inoculated) were 3wsx-3esxfor 5 min in 10 vol of lysis buffer (0.5% Nonidet P-40, 0.5% 3-[(3-cholamidopropyl)dimethylammonio]-1-propanesulfonate (CHAPS)), protease inhibitors (complete Mini, Roche), phosphatase inhibitors (PhosphoSTOP, Roche) in PBS, and centrifuged at 1000 *g* for 5 min at 4°C to remove debris prior to analysis by SDS–PAGE (Novex NuPAGE 10% Bis-Tris Gels). After electrophoresis, gel was transferred to iBlot I (Invitrogen) and transferred onto nitrocellulose membranes. Membranes were blocked in 5% Sureblock for 1 h at room temperature followed by incubation with primary antibody overnight. Membrane was washed 3x (15 min each) with PBS-Triton (0.2%) followed by incubation with HRP-tagged secondary antibody (Peroxidase-Goat Anti-Mouse IgG (H + L) (#62-6520) or Peroxidase-Goat Anti-Rabbit IgG (H + L) (#111.035.045); 1h at room temperature) and further washes (3x, 10 min). Membrane was developed with Luminata Crescendo (Millipore) and images were acquired using LAS-3000 Imaging system from FUJI. Densitometry analysis was performed using Quantity One software (BioRAD) and data were plotted using Graphpad software.

2.5 | Immunohistochemistry

Brain tissues were fixed in formalin and treated with concentrated formic acid to inactivate prions. About 2μm thick sections were prepared from these brains and deparaffinized using graded alcohols and then subjected to antigen retrieval using 10mM citrate buffer (pH 6). Astrogliosis, microgliosis, and the presence of protease-resistant prion deposits were visualized by staining brain sections with GFAP (1:1000, Agilent technologies), IBA1 (1:2500, WAKO), and the SAF84 antibody (1:200, SPI bio), respectively on a NexES immunohistochemistry robot (Ventana instruments) using an IVIEW DAB Detection Kit (Ventana). Sections were also counterstained with hematoxylin and eosin when appropriate. Images were acquired using NanoZoomer scanner (Hamamatsu Photonics) and visualized using NanoZoomer digital pathology software (NDPview; Hamamatsu Photonics). Images were acquired using Olympus BX61 Upright fluorescent microscope. Quantifications of IBA1, GFAP staining was performed on the entire brain section from the acquired images using Image J.

2.6 | Antibodies

The following antibodies are used in the current study.

Antibody	Source	Cat. No
anti-SNAP25 antibody	Abcam	ab5666
anti-GFAP	Agilent technologies	Z03344
anti-Iba1	WAKO	019-19741
anti-SAF84	Bertin bioreagent	A03208
anti-NeuN	Millipore	MAB377X
anti-calbindin	Abcam	ab108404
anti-calnexin	Enzo Life sciences	ADI-SPA-865-D
anti IL1β	Abcam	ab9722
anti-PrP^C antibodies (POM1, POM2, POM19)	Aguzzi Lab	(15)
anti-actin	Millipore	MAB1501R

2.7 | Statistical analysis

Details of the type of statistical tests performed are described in the figure legends. Results are represented as mean of replicates (μSEM). Data were analyzed using GraphPad software.

3 | RESULTS

3.1 | Generation of mice with cell type-restricted PrP^C expression

We developed a versatile transgenic mouse model that directs expression to specific cell types in a robust and controllable manner. We used a murine *Prnp* cDNA under the transcriptional control of the cytomegalovirus/chicken beta actin/rabbit beta-globin gene (CAG) promoter and a loxP-stop-loxP (LSL) cassette flanking the chloramphenicol acetyl transferase (CAT) gene [10]. When crossed to mice expressing the Cre recombinase tissue specifically, the CAT gene and the transcriptional stop cassette flanked by LoxP sites are excised, permitting activation of PrP^C expression (Figure 1A).

Pronuclear injection of the CAG-CAT-PrP construct into one-cell stage fertilized embryos from mice ablated of cellular PrP^C ($Prnp^{ZH1/ZH1}$) resulted in the generation of seven transgenic lines, four of which transmitted the transgene to their F1 offspring (Figure S1A). We next monitored the expression of CAT in brain lysates from offspring of all four transgenic lines using quantitative enzyme-linked immunosorbent assay (ELISA). Only line 211 showed sustained expression of CAT (Figure 1B). Line 211 was further bred to co-isogenic C57BL/6 *Prnp*-ablated mice ($Prnp^{ZH3/ZH3}$) for nine successive generations in order to eliminate any potential genetic confounder effects on the phenotypes observed [16].

To evaluate the robustness of CAG-CAT system in generating cell type-specific PrP^C expressors, we crossed Line 211 with mice expressing Cre under the control of the synapsin-1 (Syn) or glial fibrillary acidic protein (GFAP) promoters in order to direct PrP^C expression selectively to neurons (Syn^{Cre};loxPrP) or astrocytes ($GFAP^{Cre}$;loxPrP).

Mice were tested by ear-biopsy PCR for the CAG-CAT-PrP and the appropriate Cre transgene, and brain lysates from double-positive mice were subjected to ELISA. There were no significant differences in the expression levels of PrP^C between Syn^{Cre};loxPrP and $GFAP^{Cre}$;loxPrP mice in their brains. As expected, the overall protein levels of PrP^C were lower in brain lysates of mice expressing cell type-specific PrP^C than the wild-type mice or hemizygous $Prnp^{ZH3/+}$ mice (Figure 1C). We next sought to investigate the expression pattern of PrP^C in various brain regions of the three transgenic lines. Immunohistochemistry of entire brain sections from Syn^{Cre};loxPrP and $GFAP^{Cre}$;loxPrP mice using the anti-PrP antibody POM19 revealed differential expression of PrP^C. Syn^{Cre};loxPrP mice expressed PrP^C predominantly in the hippocampus, whereas $GFAP^{Cre}$;loxPrP mice expressed PrP^C in both cerebellum and hippocampus (Figure 1D, Figure S1B).

To further assess the cell type-restricted expression of PrP^C, we performed immunofluorescence stainings on cerebellar brain sections. Mice lacking PrP^C ($Prnp^{ZH3/ZH3}$) and wild-type mice were used as negative and positive controls. In cerebellar sections of Syn^{Cre};loxPrP mice, PrP^C expression was exclusively observed in Purkinje cells. Unlike Syn^{Cre};loxPrP mice, co-staining with MAP-2, which labels mature neuronal population, revealed that PrP^C expression in wild-type mice showed a diffuse neuronal staining. $Prnp^{ZH3/ZH3}$ mice did not show any staining of PrP^C (Figure 2A). While several glia drivers were shown to also label neuronal subpopulations [17], the GFAP-Cre driver used here was shown to exclusively label astrocytes [17]. Co-staining with GFAP in cerebellar sections of $GFAP^{Cre}$;loxPrP mice revealed astrocytic localization of PrP^C. Finally, no expression of PrP^C was seen in the absence of Cre (Figure 2B).

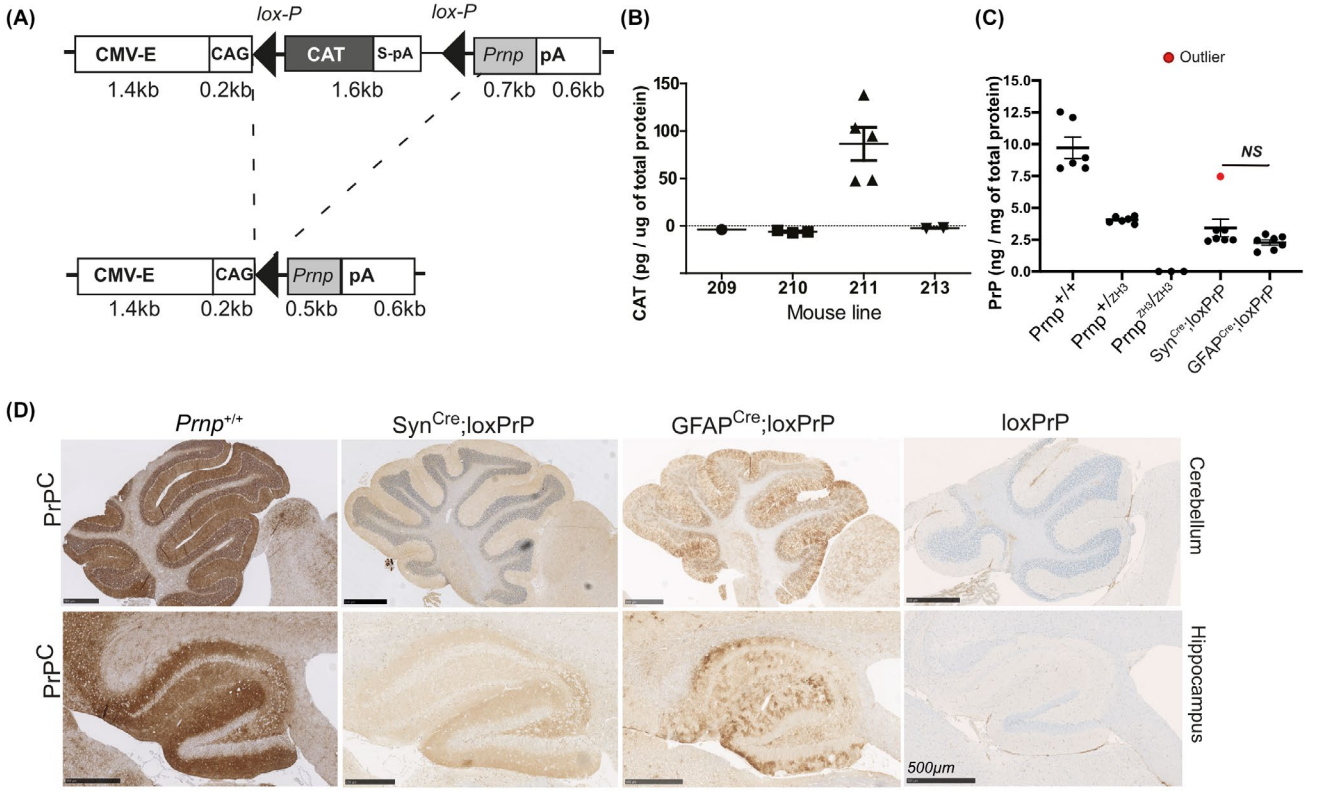

FIGURE 1 Generation and phenotyping of mice expressing PrP in defined brain compartments. (A) Schematic of the CAG-CAT-*Prnp* transgene: The transgene is driven by the CMV enhancer followed by chicken beta actin (CAG) promoter. The chloramphenicol acetyl transferase (CAT) expression cassette contains an SV40 polyadenylation signal (S-pA) and is flanked by lox-P sites, followed by the *Prnp* coding sequence and a rabbit β-globin polyadenylation signal (pA). The *Prnp* transgene is expressed only upon excision of the CAT stop sequence by the Cre recombinase. (B) Transgenic CAT expression in brain homogenates, assessed by ELISA. Assays here and in panel C were performed as triplicates; plots represent mean ± SEM. Line 211 was the only line that displayed CAT expression, and was selected for crossing with $Prnp^{ZH3/ZH3}$ mice. (C) The resulting $Prnp^{ZH3/ZH3}$;CAG-CAT-PrP mice were crossed with Cre driver lines. Brain PrP^{C} expression was compared with $Prnp^{+/+}$, $Prnp^{+/ZH}$ and $Prnp^{ZH3/ZH3}$ mice by ELISA. Crosses to Syn^{Cre} and $GFAP^{Cre}$ mice yielded mice expected to selectively express PrP^{C} in a subset of neurons and astrocytes, respectively. Dots: ELISA on individual mouse brain. Red dot: outlier Syn^{Cre};loxPrP mouse with elevated expression of PrP^{C}. Grubbs test was performed to identify the outlier. Statistics: one-way ANOVA followed by Bonferroni's post-hoc test. NS: not significant. (D) Immunohistochemistry of brain sections of Syn^{Cre};loxPrP and $GFAP^{Cre}$;loxPrP mice with anti-PrP^{C} antibody POM2. Negative and positive controls: loxPrP and wild-type mice brain sections. PrP^{C} was found mainly in the hippocampus of Syn^{Cre};loxPrP mice, whereas $GFAP^{Cre}$;loxPrP mice showed prominent staining in both hippocampus and cerebellum

3.2 | Role of neuronal and astrocytic PrP^{C} in the manifestation of prion disease

We sought to investigate the kinetics and the manifestation of prion disease in the newly generated mice expressing PrP^{C} in a subset of neurons [18]. Five Syn^{Cre};loxPrP mice were intracerebrally inoculated with prions (Rocky Mountain Laboratory strain, passage #6, henceforth termed RML6). For control, we used wild-type C57BL6/J mice, mice transgenic for Syn^{Cre} but not for loxPrP, and vice versa. Syn^{Cre};loxPrP mice developed clinical scrapie, albeit with significantly longer incubation times than wild-type mice (435 vs 196 days after inoculation (dpi), respectively, $p = 0.002$) (Figure 3A). Hence neuronal PrP^{C} expression suffices to confer susceptibility to prion disease. We next assessed proteinase K (PK)-resistant prion protein (termed PrP^{Sc}) in brain lysates of terminally scrapie-sick wild-type and Syn^{Cre};loxPrP mice, as well as age-matched loxPrP, Syn^{Cre} or $Prnp^{ZH3/ZH3}$ mice. Western blotting of PK-treated lysates (25 µg/ml, 37°C, 1h) revealed PrP^{Sc} only in wild-type and Syn^{Cre};loxPrP lysates (Figure 3B). Next, five $GFAP^{Cre}$;loxPrP transgenic mice were inoculated intracerebrally with RML6 prions. For control we used wild-type mice, $GFAP^{Cre}$ mice, loxPrP mice, and $Prnp^{ZH3/ZH3}$ mice. Over a period of 627 dpi, neither $GFAP^{Cre}$;loxPrP mice nor $Prnp^{ZH3/ZH3}$ mice developed any signs of scrapie, whereas $Prnp^{+/+}$ mice (with or without Cre transgenes) developed terminal scrapie at 167 ± 5 dpi (Figure 3C). Western blots showed similar amounts of PrP^{Sc} in terminally scrapie-sick wild-type mice and in 2-year-old prion-infected $GFAP^{Cre}$;loxPrP mice (627 dpi) (Figure 3D).

Histological analysis of hippocampal and cerebellar brain sections revealed vacuolation (spongiosis) in Syn^{Cre};loxPrP mice, albeit less pronounced than in wild-type mice, whereas $GFAP^{Cre}$;loxPrP did not show any vacuolation (Figure 3E). Immunohistochemistry with anti-PrP antibody, SAF84 [19]

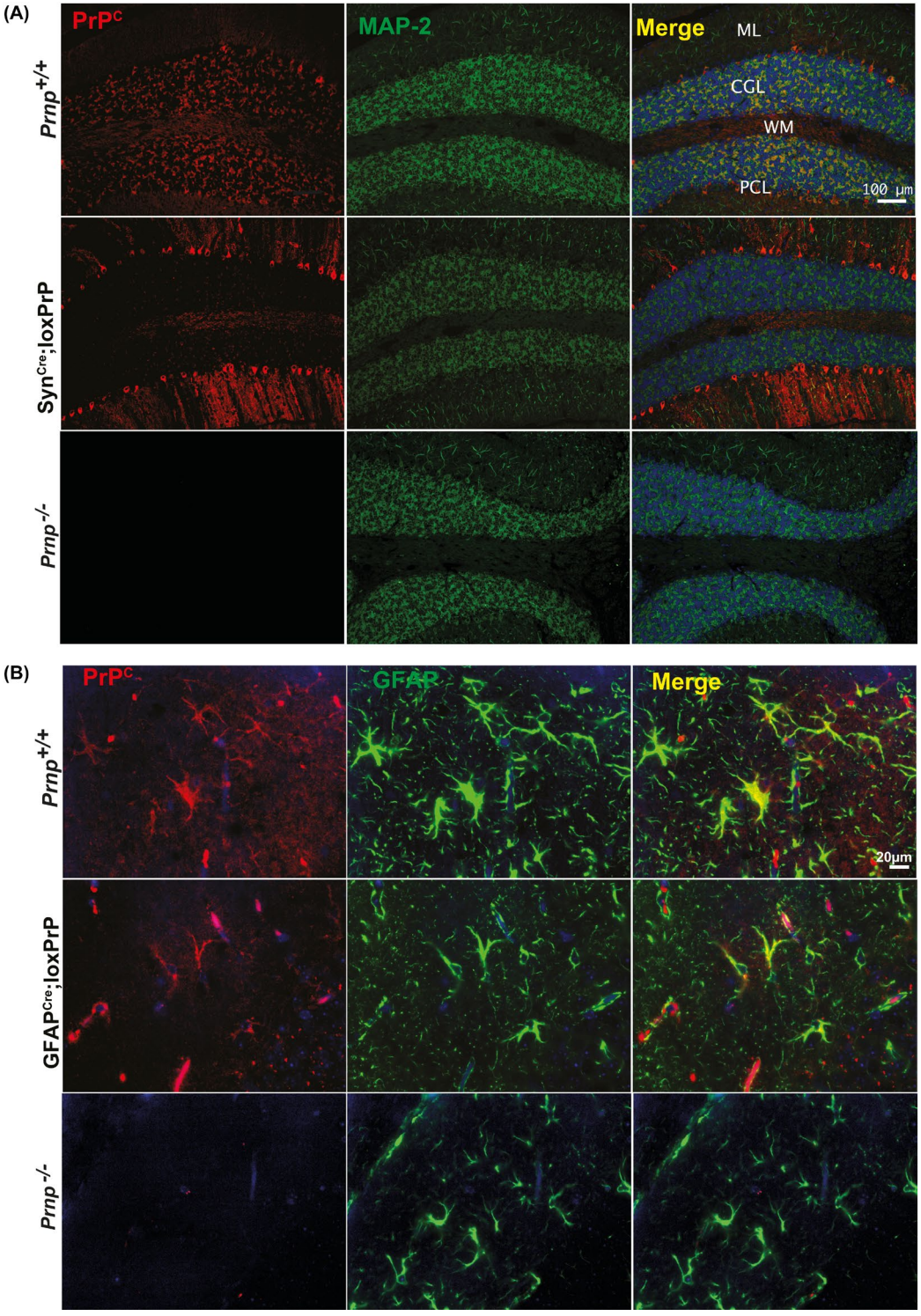

FIGURE 2 PrP^C expression patterns in CAG-CAT-PrP mice. (A and B) Cerebellar sections of wild-type and transgenic mice (as indicated) were immunostained for PrP^C (red) as well as for MAP2 (microtubule-associated protein 2), GFAP (glial fibrillary acidic protein), which were used as neuronal and astrocytic markers, respectively (green). As controls cerebellar sections from Prnp ablated mice were used. Blue: cell nuclei (DAPI). In *Prnp*$^{+/+}$ mice, PrP^C is detected in the cerebellar granule cell layer (CGL), Purkinje cells (PCL), and molecular layer (ML). In Syn^{Cre};loxPrP cerebella (A), PrP^C was mostly detected in Purkinje cells. In $GFAP^{Cre}$;loxPrP, PrP^C was exclusively detected in astrocytes colocalizing with GFAP. *Prnp* ablated mice revealed absence of any unspecific staining. Each staining was performed on sections from at least three individual mice

in hippocampal sections of Syn^{Cre};loxPrP mice revealed the presence of PrP deposits, albeit at lower amounts than in wild-type mice, while mice lacking PrP or Cre-recombinase did not show any staining (Figure 3E). Syn^{Cre};loxPrP mice, which expressed PrP^C predominantly in Purkinje cells, exhibited fewer PrP deposits than wild-type mice

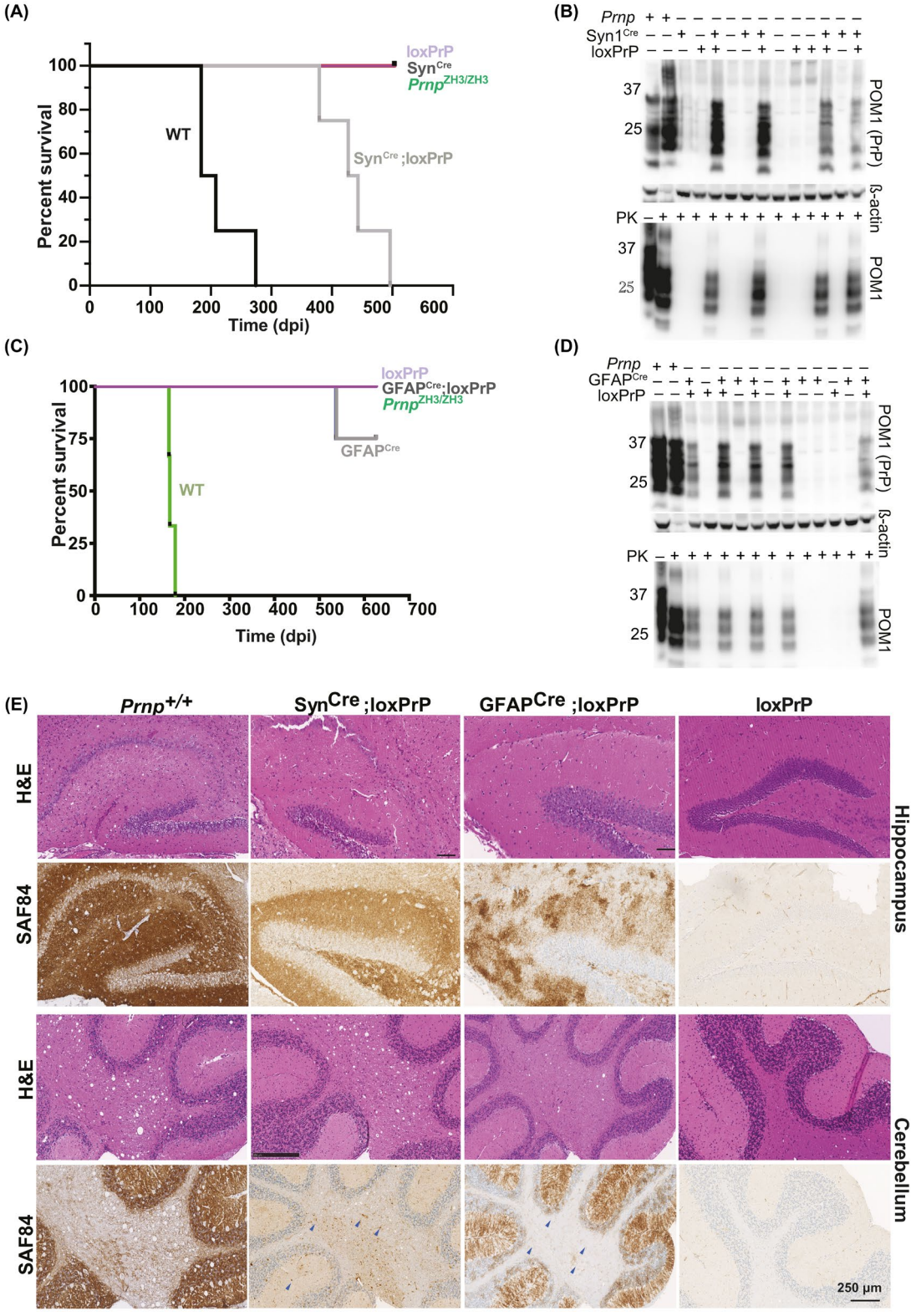

(Figure 3E). SAF84 immunostaining in prion inoculated GFAP^{Cre};loxPrP mice however revealed PrP deposits in both cerebellum and hippocampus (Figure 3E). Taken together, these results suggest that mice with neuron-restricted PrP^{C} develop clinical and histological features of prion disease whereas PrP^{C} expression in astrocytes alone does not lead to prion disease, yet it supports PrP^{Sc} accumulation.

3.3 | Astrocyte-restricted PrP^{C} does not induce neurodegeneration in COCS

We next generated cerebellar organotypic cultured slices (COCS) from 8-day-old Syn^{Cre};loxPrP mice and inoculated them with RML6 prions or with non-infectious brain homogenate (NBH). At 56 dpi, these COCS were

FIGURE 3 Neuron-selective, but not astrocyte-selective, PrP^C expression confers susceptibility to prion disease. (A) Survival of Syn^{Cre};loxPrP, loxPrP, Syn^{Cre}, $Prnp^{ZH3/ZH3}$ and wild-type mice inoculated intracerebrally with RML6 prions. The median incubations for Syn^{Cre-};loxPrP (n = 5) and wild-type mice (n = 4) were 435 and 195 days post inoculation (dpi), respectively. Survival curves were compared by a log-rank (Mantel-Cox) test. (B) Total PrP (upper panel) and PK-resistant PrP^{Sc} (lower panel) in brains of prion-infected, terminally sick mice. Syn^{Cre};loxPrP and wild-type brains, but not loxPrP brains, contained PrP^{Sc}. β-actin: loading control. Lane #2 (upper panel) was intentionally underloaded to avoid overexposure. (C) Survival curves of $GFAP1^{Cre}$;loxPrP, loxPrP, $Prnp^{ZH3/ZH3}$ and wild-type mice inoculated with RML6 prions intracerebrally. $GFAP^{Cre}$;loxPrP (n = 5) did not develop clinical signs of prion disease. Wild-type mice (n = 4): 167 dpi (median incubation time). One of the $GFAP^{Cre}$ mice was sacrificed (544 dpi) because of acute dermatitis and did not exhibit scrapie signs or PrP^{Sc} accumulation. (D) Western blot of total PrP and PK-digested PrP^{Sc} in brain homogenates of prion-infected $GFAP^{Cre}$;loxPrP (627 dpi) and control mice. $GFAP^{Cre}$;loxPrP harbor copious PrP^{Sc}. (E) Hippocampal and cerebellar histology of prion-infected Syn^{Cre};loxPrP, $GFAP^{Cre}$;loxPrP, loxPrP, and $Prnp^{+/+}$ mice. Slices were stained with hematoxylin and eosin (H&E) and anti-PrP antibody SAF84. Both astrocyte- and neuron-restricted PrP transgenic mice accumulated PrP^{Sc}, but their deposition patterns differed profoundly. Blue arrows in cerebellar regions of Syn^{Cre};loxPrP and $GFAP^{cre}$;loxPrP: PrP^{Sc} deposits

immunostained with NeuN (staining cerebellar granule cells) and calbindin (staining Purkinje cells) [20].

Neuronal loss in COCS was measured by morphometric assessment of cerebellar granule layer (CGL) area immunoreactive to the antibodies against NeuN and calbindin. COCS generated from Syn^{Cre};loxPrP mice showed a significant decrease in calbindin staining, confirming neurodegeneration of PrP expressing Purkinje cells in the Syn^{Cre};loxPrP mice. Surprisingly, there was also a significant loss of afferent $NeuN^+$ cerebellar granule neurons, possibly due to secondary effects arising from Purkinje cell death [21]. In contrast, control COCS from loxPrP mice did now show any neurodegeneration (Figure 4A).

To further challenge the conclusion that astrocyte-restricted PrP^C expression does not restore prion-dependent neurodegeneration, we generated COCS from 9-day-old pups of $GFAP^{Cre}$;loxPrP and for control from loxPrP mice. COCS were inoculated with RML6 prions or NBH. At 56dpi COCS were subjected to immunostaining with NeuN. COCS from $GFAP^{Cre}$;loxPrP did not show any signs of neuronal loss (Figure 4B). We next investigated if COCS from $GFAP^{Cre}$;loxPrP are also resistant to prion mimetics. COCS from 9–day-old $GFAP^{Cre}$;loxPrP mice were treated with the prion-mimetic antibody POM1 or with pooled mouse IgG, fixed after 10 days of treatment, and immunostained with NeuN and calbindin. As controls, COCS were generated from *tga*20 (mice overexpressing PrP^C) [22] and loxPrP mice were used. COCS from *tga20* mice, but not from $GFAP^{Cre}$;loxPrP and loxPrP mice, showed conspicuous neuronal loss (Figure 4C).

3.4 | Mice with neuron or astrocyte restricted PrP^C expression do not activate microglia upon prion infection.

Prion diseases typically feature extreme activation and proliferation of microglia to an extent rarely seen in any other brain diseases. We assessed the status of microglia and astrocytes by immunohistochemistry for Iba1 and GFAP on the cortical and hippocampal brain sections of terminally scrapie-sick wild-type mice and Syn^{Cre};loxPrP mice. For control, we used loxPrP mice. While wild-type mice showed a high microglia density, we were surprised to find that Syn^{Cre};loxPrP mice did not show more microglial activation and astrogliosis than control mice (Figure 5A–C, Figure S2A) despite being terminally scrapie-sick. We performed the same analysis in prion-infected $GFAP^{Cre}$;loxPrP mice. Also here, the staining of cortical and hippocampal sections with anti-Iba1 and anti-GFAP did not reveal any microglia activation or astrogliosis beyond the baseline of control mice ($GFAP^{Cre-}$;loxPrP, $GFAP^{Cre}$;$loxPrP^-$), whereas wild-type mice showed a brisk enhancement of Iba1 and GFAP immunoreactivity (Figure 5A-C, Figure S2A).

3.5 | Molecular changes associated with microglial activation remain unaltered in mice with cell type restricted PrP^C upon prion infection

Microglial changes typically precede the onset of the clinical signs of the disease, and are accompanied by the expression of pro-inflammatory cytokines such as TNFa, IL1α, and IL1β. Hemispheric brain lysates from the same prion-infected mice as above were then subjected to western blotting to monitor the expression of SNAP25 (a presynaptic protein engulfed by microglia previously shown to be reduced in prion infections before the onset of motor defects [23]), GFAP, IL-1β, and Iba-1. Terminally scrapie-sick wild-type mice showed a substantial increase in the expression of GFAP, Iba-1, and IL-1β, whereas Syn^{Cre};loxPrP and $GFAP^{Cre}$;loxPrP lysates were similar to the negative controls. Only SNAP-25 was slightly elevated in Syn^{Cre};loxPrP mice (Figure 5D,E). These results indicate that microglial activation is not induced by prion infection in mice expressing PrP^C only in neurons or astrocytes.

3.6 | Prion infection does not elicit its transcriptional signature in mice expressing astrocyte-restricted PrP^C

Previous studies have longitudinally mapped transcriptional changes associated with prion disease in

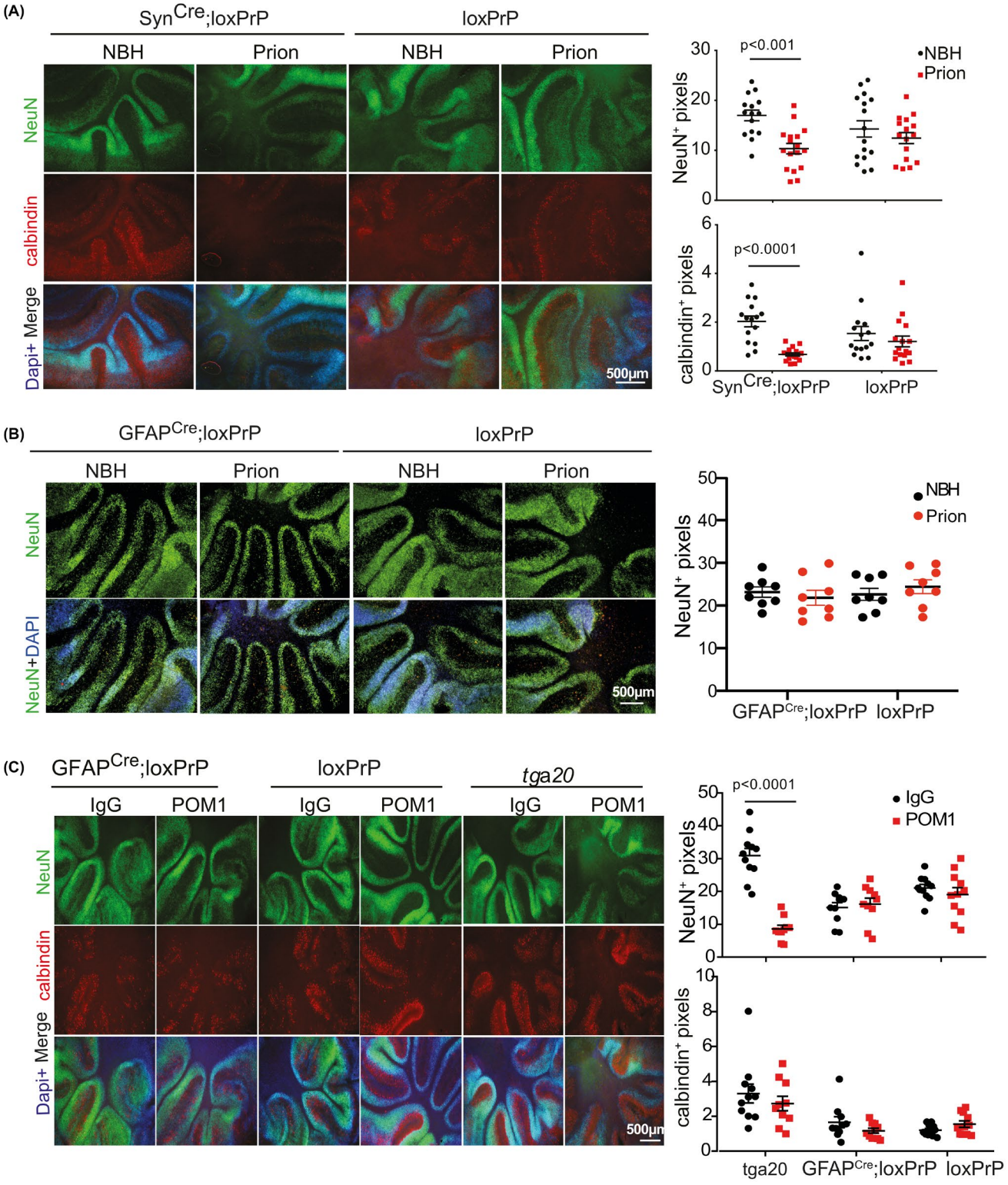

FIGURE 4 COCS from astrocyte-restricted PrP^C mice are resistant to neurodegeneration induced by prion mimetics. (A) Fluorescence micrographs of cerebellar organotypic cultured slices (COCS) of Syn^{Cre};loxPrP and loxPrP COCS infected with prions (56 dpi) or exposed to noninfectious brain homogenate (NBH). Purkinje cells were identified by calbindin immunostaining. Calbindin and NeuN morphometry (right) shows degeneration of granule and Purkinje cells in prion-infected Syn^{Cre};loxPrP COCS. Each dot represents a cerebellar slice. Here and henceforth: one-way ANOVA was used for statistical analysis. (B) Fluorescence micrographs of GFAP^{Cre};loxPrP and loxPrP COCS infected with prions or exposed to non-infectious brain homogenate (NBH). Slices were cultured for 56 days and stained with anti-NeuN antibody. There was no discernible loss of NeuN signal in prion-infected COCS. For control, we stained COCS from loxPrP mice. Right panel: quantification. Each dot represents a cerebellar slice. One-way ANOVA was used for statistical analysis; NS: not significant. Nuclei were stained with DAPI. (C) Fluorescence micrographs of GFAP^{Cre};loxPrP, loxPrP, and *Tga*20 COCS exposed to the neurotoxic anti-PrP antibody POM1 or IgG control and cultured for 10 days were stained for NeuN (green), calbindin (red), and DAPI (blue). POM1 did not trigger neuronal loss in GFAP^{Cre};loxPrP COCS, whereas neurodegeneration was extensive in *Tga*20 COCS. Each dot represents a cerebellar slice

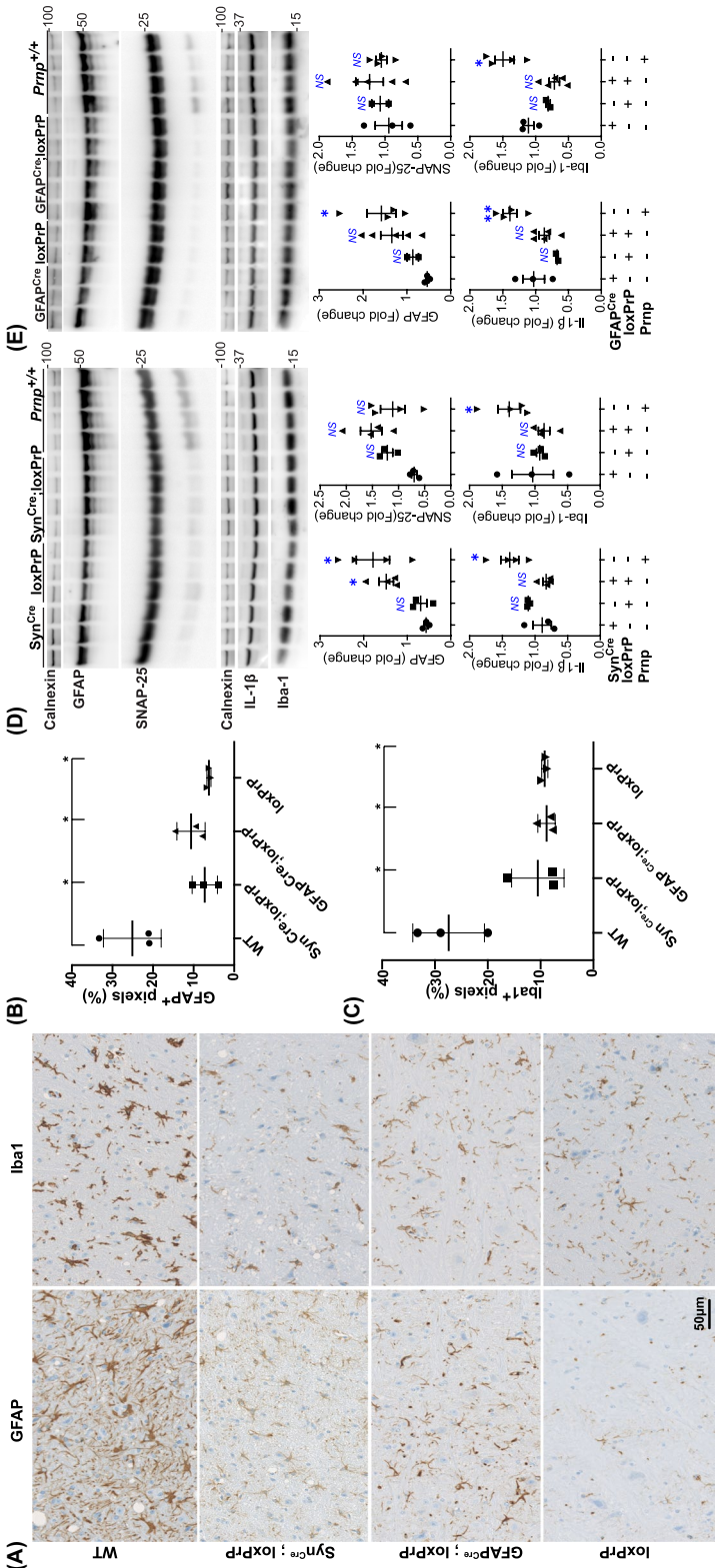

FIGURE 5 Prion infection of neuron and astrocyte-specific PrP expressors does not induce microglia activation. (A) Microglia (Iba1) and astrocyte (GFAP) immunostains of the cortical sections of prion-inoculated Syn^{Cre};loxPrP (379 dpi), GFAP^{Cre};loxPrP (627 days), loxPrP (504 dpi), and wild-type (184 dpi) mice. (B and C) Quantification of GFAP^{+} (B) and Iba1^{+} (C) pixels in a cross-section of complete mouse brain. Expression of both markers was conspicuously increased in *Prnp*$^{+/+}$ mice, whereas Syn^{Cre};loxPrP and GFAP^{Cre};loxPrP revealed significantly lower amounts of GFAP and Iba1. Each dot represents quantification performed on brain sections obtained from an individual mouse. Statistics: one-way Anova test. (D and E) Western blot analysis of brain lysates generated from the enrire hemispheres and related quantification of GFAP, SNAP-25, IL1-Beta, and Iba-1 in prion inoculated Syn^{Cre};loxPrP mice (D) and GFAP^{Cre};loxPrP mice (E) versus controls. Calnexin was used for loading control. Only SNAP-25 showed elevated expression in prion-infected Syn^{Cre};loxPrP mice, whereas all other markers of microglial activation remained unaltered. Each dot represents data from lysate obtained from an individual mouse. Statistics: one-way Anova test

mice, and revealed changes in gene expression from as early as 4 weeks post prion infection [8]. We asked if GFAP^{Cre};loxPrP mice, which do not develop clinical signs after prion infection, exhibit transcriptional changes upon prion infection. Three GFAP^{Cre};loxPrP mice were intracerebrally inoculated with RML6 prions; for control we inoculated two GFAP^{Cre};loxPrP mice with non-infectious brain homogenate (NBH). Prion-infected mice did not manifest prion disease and were humanely euthanized along with the NBH-treated mice at approximately 627 dpi. RNA was isolated from cerebella of these mice and processed for RNA sequencing (Figure 6A). Unsupervised clustering of the 100 genes with highest variance across all the samples did not reveal any separation between the prion-infected and NBH-treated samples (Figure 6B). Data analysis to identify differentially expressed genes (DEGs) in prion inoculated vs NBH-treated mice revealed absence of any DEGs when a filter of Log_2FC >0.5 and FDR <0.05 was applied (Figure 6A). We then relaxed the stringency by applying a filter of Log_2FC >0.5 and *p*-value <0.05. This revealed 168 DEGs in prion inoculated GFAP^{Cre};loxPrP mice. Of the 168 DEGs, 104 genes were upregulated, and 64 genes were downregulated (Figure 6C, Table S1). Functional gene ontology studies revealed upregulated genes were enriched in biological processes associated with hormonal response pathways (Figure S2B), whereas the downregulated genes were not enriched in any pathway. A total of 3723 genes were previously shown to have their expression altered at least at one measured time point

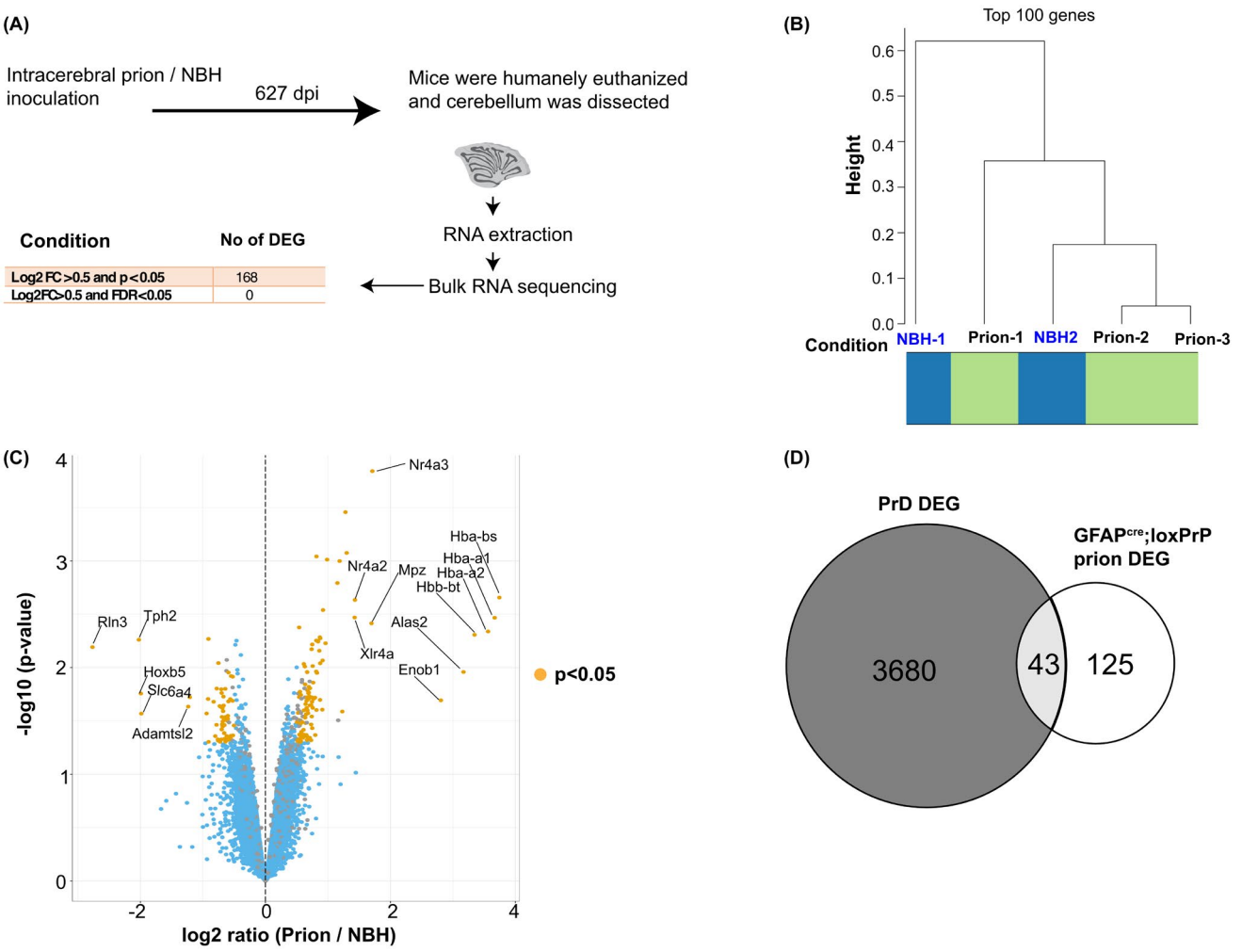

FIGURE 6 Prion disease-specific transcriptional signature is absent in astrocyte-specific PrP^{C} expressors infected with prions. (A) Schematic representation of the sample collection (cerebellum) and bulk RNA sequencing after prion or NBH inoculation of GFAP^{Cre};loxPrP mice. The number of differentially expressed genes (DEGs) and the filtering criteria used to derive them are indicated. (B) Hierarchical clustering analysis based on the 100 genes with highest variance across all the samples did not reveal a separation between NBH and prion-infected mice ($n = 3$ for prion inoculations and $n = 2$ for NBH injections). (C) Volcano plot showing differentially expressed genes in the prion inoculated GFAP^{Cre};loxPrP mice compared with the NBH-injected counterparts. Genes with Log_2FC >0.5 and *p*-value <0.05 were considered as DEGs. The identities of the top 10 upregulated and top 5 downregulated genes are reported in the plot. Log_2FC: log twofold change. (D) Intersection between the DEGs observed during the progression of prion disease in C57BL6/J mice (3723 genes) and DEGs in prion inoculated GFAP^{Cre};loxPrP mice (168 genes). The intersection consists of only 43 genes, suggesting that prion-infected GFAP^{Cre};loxPrP mice do not exhibit any prion-specific transcriptomic signature

during the course of prion disease in C57BL6/J mice inoculated with RML6 prions. We next tested if any of the DEGs from the prion-inoculated $GFAP^{Cre}$;loxPrP mice overlapped with the DEGs observed during the progression of prion disease in C57BL6/J mice. Intersection plots revealed that 43 genes with altered expression in $GFAP^{Cre}$;loxPrP mice were also differentially expressed during the prion disease (Figure 6D, Table S2). These 43 DEGs however did not correlate with any particular time point during the progression of prion disease. We deduce that PrP^{Sc} produced by astrocytes does not induce the transcriptional changes typical of prion diseases.

4 | DISCUSSION

While many transgenic mouse lines with tissue-specific PrP^{C} expression have been generated in the past two decades, we still lack a flexible generic model system allowing for expression in any given cell type under highly controlled conditions. What is worse, several of the transgenic models alleged to display cell-specific PrP^{C} expression in reality exhibit illegitimate expression in ectopic compartments: the widely used neuron-specific enolase (NSE) promoter can be expressed in glial cells [24] and earlier versions of a GFAP-driven construct are expressed in neurons [25, 26]. This situation has motivated us to generate the lines described in this study. We opted to use the CAG-CAT system [10] and in its native state, the CAG-CAT transgene leads to sustained and ubiquitous expression of chloramphenicol acetyl transferase (CAT), whose presence can be easily monitored with an enzyme activity assay. Upon CRE-mediated recombination, the loxP-flanked CAT minigene and its polyadenylation signal are excised, and transcription of PrP^{C} is enabled. We tested the system with two CRE-expressor crossings directing PrP^{C} expression to neurons and astrocytes. We chose the Synapsin-1 promoter as it is selectively, but broadly expressed in many types of neurons. Conversely, the mGFAP line 77.6 used in the current study has previously been shown to express Cre exclusively in astrocytes [17]. Although expressed in different cell types, PrP^{C} expression in these lines remained comparable.

The data reported here enable new insights into two aspects of prion pathology: cell type-specific replication and cell type-specific toxicity. The expression of PrP^{C} is a necessary but insufficient prerequisite to prion replication, and multiple cell types replicate prions during their journey from the periphery to the brain. However, many tissues do not replicate prions despite expression of PrP^{C}. While the replication competence of neurons is well established, the data on astrocytes have remained controversial. One of us (AA) reported that mice expressing hamster PrP^{C} off a GFAP promoter would replicate prions and develop disease [27]. However, a similar construct was found to be active ectopically in certain populations of neurons, raising the possibility of low-level expression of the transgene and thereby [25] raising doubts on the validity of the previous report. The GFAP-Cre line used in the current study, unlike the previous GFAP promoter-derived constructs has no expression in the postnatal or adult neural stem cells or their progeny [17]. The specificity of transgenic mice described in the current study is arguably more stringent. Although these mice did not develop any histological signs of neuroinflammation and clinical disease, we confirmed that astrocytes are capable of prion replication and PrP^{Sc} deposition in vivo.

The terminal stage of prion diseases is typically characterized by extensive neuronal loss. This observation has led to the implicit assumption that neurons are the primary targets, and possibly the primary driver, of prion diseases. An impressive panoply of evidence has accumulated that neuronal damage is crucially dependent on expression of PrP^{C} by the neurons targeted by prions. The first hint came from grafting PrP^{C}-expressing neural tissue into PrP^{C}-deficient mice. After prion infection, grafts developed all the pathological features of prion disease, yet no damage was observed in the adjoining tissue lacking PrP^{C} despite PrP^{Sc} deposition loss [28, 29]. An additional line of evidence came from partial depletion of neuronal PrP^{C}, which decelerated the development of disease despite deposition of PrP^{Sc} [7]. Furthermore, transgenic mice expressing a hamster prion protein in neurons became susceptible to prion disease after exposure to hamster prion, suggesting that mere expression of PrP^{C} in neurons suffices to develop prion disease [30].

On the other hand, a growing number of observations is challenging the perception that neurons are the sole, or even the dominant, cellular actor in prion pathology. Recently concluded longitudinal transcriptomic study mapping the changes in gene expression during the course of prion infection has revealed that glial perturbations occur simultaneously to the onset of clinical disease. Surprisingly, no changes in the expression of neuron-enriched transcript were detectable at this time point. Instead, suppression of neuronal transcripts was only observed at the terminal stage of disease [8]. The onset of changes associated with actively translating genes during the course of prion infection also revealed glial perturbation as the major contributors in driving the course of prion disease [9]. More importantly, disease-associated microglia (DAM) genes and A1 astrocytes, both of which are renowned glia signatures in several neurodegenerative diseases were upregulated in prion disease. Overall, these studies revealed an important role for non-neuronal cell types in the manifestation of prion disease.

4.1 | Contribution of cell type-specific PrP^{C} to prion disease

Prion inoculated Syn^{Cre};loxPrP mice displayed all the characteristic histopathological and clinical features of

prion disease. The incubation time was much longer than that of wild-type mice (median survival: 435 vs 196 days), which may be explained by the lower total brain PrP^{C} concentration.

Although the mechanisms responsible for neuronal death are yet to be elucidated, it is evident that PrP^{Sc} deposits from non-neuronal counterparts could accelerate the conversion of neuronal PrP^{C} and thereby aggravating neuronal loss. Interestingly, these mice showed no activation of microglia and astrocytes and this further confirms the hypothesis that glial activation drives the progression of the disease and in its absence the onset of the disease follows a much longer time course. One interesting question that arises is whether the glial activation in prion disease requires the presence of PrP^{C} in both neurons and astrocytes and what is the interplay between neurons and astrocytes? Studies have pointed out toward an important role for neurons and neuronal activity not only in determining astrocytic fate but also how they can be potentially altered in neurodegeneration [31]. The Syn^{Cre};loxPrP mice line delinks glial activation from neuronal death and could be potentially used as a model system to study the mechanisms associated with neuronal death in prion disease.

Among non-neuronal cells, astrocytes are the cell type producing highest amount of PrP^{C} [32] followed by oligodendrocytes. Previous studies have shown astrocytes are not only capable of replicating and propagating prions but also can deposit PrP^{Sc} aggregates [27], whereas PrP^{C} expression restricted to myelinating cells failed to accumulate PrP^{Sc} or develop prion disease [33]. Transgenic mice expressing PrP^{C} exclusively in astrocytes ($GFAP^{Cre;}$loxPrP) do not develop prion disease and do not show any of the classical pathological features apart from deposition of PrP^{Sc}. These mice also fail to recapitulate glia activation or upregulate any of the inflammation markers. RNA sequencing data corroborated the absence of molecular markers of disease. Differentially expressed genes became identifiable only when the stringency of the analysis was substantially relaxed, and even then they did not appear to be enriched in any specific cell types or pathways. We conclude that astrocyte-selective prion infection has remarkably bland effects on the brain.

In a previous study, mice expressing PrP^{C} under the expression of GFAP promoter were shown to replicate prions but did not develop scrapie [34]. The capability of astrocytes to replicate prions was however questioned because the GFAP promoter fragment used to generate the mice also exhibited partial neuronal expression [25, 26]. With the newly generated mouse models described here, we have confirmed that astrocytes are indeed capable of replicating prions. These findings vindicate a report that cultured iPSC-derived astrocytes can replicate CJD prions [35]. Furthermore, a recent study has documented the transport of PrP^{Sc} from astrocytes to neurons, suggesting a noncell-autonomous mechanism of toxicity [36]. The results presented here argue that this is not the case and that accumulation and transport of astrocytic PrP^{Sc} does not suffice to induce neurotoxicity.

In the future, these newly generated mice lines can help answering some of the long-standing questions in the prion field and may represent ideal tools to delineate the role and contribution of each of the cell types in manifestation of prion disease.

ACKNOWLEDGMENTS

The authors thank Mirzet Delic and Paulina Pawlak for animal husbandry, and Merve Avar for help with data analysis of RNA sequencing data. AA is the recipient of an Advanced Grant of the European Research Council (ERC 670958), the Swiss National Foundation (SNF: 179040), the Nomis Foundation and SystemsX.ch. AS, SS, and AKKL are recipients of a grant from the Synapsis Foundation.

CONFLICT OF INTEREST

The authors declare no competing financial interests.

AUTHOR CONTRIBUTIONS

Adriano Aguzzi initiated and supervised the project, and wrote the manuscript. Asvin K. K. Lakkaraju performed RNA sequencing experiment, analyzed all the data, and wrote the manuscript. Assunta Senatore performed slice cultures, immunohistochemistry, ELISA, western blots, and analyzed the data. Silvia Sorce contributed to generation of mice lines, immunohistochemistry, ELISA, and analyzed the data. Mario Nuvolone contributed to generation of mice lines. Jingjing Guo, Petra Schwarz, Rita Moos provided the technical help in performing all the experiments in the manuscript. Pawel Pelczar performed microinjections and contributed to the generation of mice lines. All authors have read and approved the final version of the manuscript.

MATERIAL AVAILABILITY

All unique reagents used for this study will be available from the lead contact upon request with a material transfer agreement.

DATA AVAILABILITY STATEMENT

All original data have been included in the article. Uncropped western blots from the entire manuscript are included in Figure S3. No cropping was performed on any of the microscopy images. Any additional information/data required will be made available by the corresponding author upon reasonable request. No source code was generated in this study.

ORCID

Asvin K. K. Lakkaraju https://orcid.org/0000-0001-8752-148X
Silvia Sorce https://orcid.org/0000-0002-3843-8644
Assunta Senatore https://orcid.org/0000-0003-0144-1476
Jingjing Guo https://orcid.org/0000-0002-2411-0082

Pawel Pelczar https://orcid.org/0000-0003-0189-6868
Adriano Aguzzi https://orcid.org/0000-0002-0344-6708

REFERENCES

1. Aguzzi A. Cell biology: Beyond the prion principle. Nature. 2009;459(7249):924–5.
2. Bueler H, Aguzzi A, Sailer A, Greiner RA, Autenried P, Aguet M, et al. Mice devoid of PrP are resistant to scrapie. Cell. 1993;73(7):1339–47.
3. Brandner S, Isenmann S, Raeber A, Fischer M, Sailer A, Kobayashi Y, et al. Normal host prion protein necessary for scrapie-induced neurotoxicity. Nature. 1996;379(6563):339–43.
4. Brandner S, Raeber A, Sailer A, Blattler T, Fischer M, Weissmann C, et al. Normal host prion protein (PrPC) is required for scrapie spread within the central nervous system. Proc Natl Acad Sci U S A. 1996;93(23):13148–51.
5. Aguzzi A, Nuvolone M, Zhu C. The immunobiology of prion diseases. Nat Rev Immunol. 2013;13(12):888–902.
6. Budka H. Neuropathology of prion diseases. Br Med Bull. 2003;66:121–30.
7. Mallucci G, Dickinson A, Linehan J, Klohn PC, Brandner S, Collinge J. Depleting neuronal PrP in prion infection prevents disease and reverses spongiosis. Science. 2003;302(5646):871–4.
8. Sorce S, Nuvolone M, Russo G, Chincisan A, Heinzer D, Avar M, et al. Genome-wide transcriptomics identifies an early preclinical signature of prion infection. PLoS Pathog. 2020;16(6):e1008653.
9. Scheckel C, Imeri M, Schwarz P, Aguzzi A. Ribosomal profiling during prion disease uncovers progressive translational derangement in glia but not in neurons. eLife. 2020;9:e62911.
10. Araki K, Araki M, Miyazaki J, Vassalli P. Site-specific recombination of a transgene in fertilized eggs by transient expression of Cre recombinase. Proc Natl Acad Sci U S A. 1995;92(1):160–4.
11. Henzi A, Senatore A, Lakkaraju AKK, Scheckel C, Muhle J, Reimann R, et al. Soluble dimeric prion protein ligand activates Adgrg6 receptor but does not rescue early signs of demyelination in PrP-deficient mice. PLoS One. 2020;15(11):e0242137.
12. Robinson MD, McCarthy DJ, Smyth GK. edgeR: a Bioconductor package for differential expression analysis of digital gene expression data. Bioinformatics. 2010;26(1):139–40.
13. Falsig J, Aguzzi A. The prion organotypic slice culture assay–POSCA. Nat Protoc. 2008;3(4):555–62.
14. Sonati T, Reimann RR, Falsig J, Baral PK, O'Connor T, Hornemann S, et al. The toxicity of antiprion antibodies is mediated by the flexible tail of the prion protein. Nature. 2013;501(7465):102–6.
15. Polymenidou M, Moos R, Scott M, Sigurdson C, Shi YZ, Yajima B, et al. The POM monoclonals: a comprehensive set of antibodies to non-overlapping prion protein epitopes. PLoS One. 2008;3(12):e3872.
16. Nuvolone M, Hermann M, Sorce S, Russo G, Tiberi C, Schwarz P, et al. Strictly co-isogenic C57BL/6J-Prnp-/- mice: a rigorous resource for prion science. J Exp Med. 2016;213(3):313–27.
17. Gregorian C, Nakashima J, Le Belle J, Ohab J, Kim R, Liu A, et al. Pten deletion in adult neural stem/progenitor cells enhances constitutive neurogenesis. J Neurosci. 2009;29(6):1874–86.
18. Zhu Y, Romero MI, Ghosh P, Ye Z, Charnay P, Rushing EJ, et al. Ablation of NF1 function in neurons induces abnormal development of cerebral cortex and reactive gliosis in the brain. Genes Dev. 2001;15(7):859–76.
19. Demart S, Fournier JG, Creminon C, Frobert Y, Lamoury F, Marce D, et al. New insight into abnormal prion protein using monoclonal antibodies. Biochem Biophys Res Commun. 1999;265(3):652–7.
20. Weyer A, Schilling K. Developmental and cell type-specific expression of the neuronal marker NeuN in the murine cerebellum. J Neurosci Res. 2003;73(3):400–9.
21. Doughty ML, De Jager PL, Korsmeyer SJ, Heintz N. Neurodegeneration in Lurcher mice occurs via multiple cell death pathways. J Neurosci. 2000;20(10):3687–94.
22. Fischer M, Rulicke T, Raeber A, Sailer A, Moser M, Oesch B, et al. Prion protein (PrP) with amino-proximal deletions restoring susceptibility of PrP knockout mice to scrapie. EMBO J. 1996;15(6):1255–64.
23. Moreno JA, Radford H, Peretti D, Steinert JR, Verity N, Martin MG, et al. Sustained translational repression by eIF2alpha-P mediates prion neurodegeneration. Nature. 2012;485(7399):507–11.
24. Kugler S, Kilic E, Bahr M. Human synapsin 1 gene promoter confers highly neuron-specific long-term transgene expression from an adenoviral vector in the adult rat brain depending on the transduced area. Gene Ther. 2003;10(4):337–47.
25. Marino S, Vooijs M, van Der Gulden H, Jonkers J, Berns A. Induction of medulloblastomas in p53-null mutant mice by somatic inactivation of Rb in the external granular layer cells of the cerebellum. Genes Dev. 2000;14(8):994–1004.
26. Zhuo L, Theis M, Alvarez-Maya I, Brenner M, Willecke K, Messing A. hGFAP-cre transgenic mice for manipulation of glial and neuronal function in vivo. Genesis. 2001;31(2):85–94.
27. Raeber AJ, Race RE, Brandner S, Priola SA, Sailer A, Bessen RA, et al. Astrocyte-specific expression of hamster prion protein (PrP) renders PrP knockout mice susceptible to hamster scrapie. EMBO J. 1997;16(20):6057–65.
28. Brandner S, Klein MA, Frigg R, Pekarik V, Parizek P, Raeber A, et al. Neuroinvasion of prions: insights from mouse models. Exp Physiol. 2000;85(6):705–12.
29. Glatzel M, Aguzzi A. PrP(C) expression in the peripheral nervous system is a determinant of prion neuroinvasion. J Gen Virol. 2000;81(Pt 11):2813–21.
30. Race RE, Priola SA, Bessen RA, Ernst D, Dockter J, Rall GF, et al. Neuron-specific expression of a hamster prion protein minigene in transgenic mice induces susceptibility to hamster scrapie agent. Neuron. 1995;15(5):1183–91.
31. Hasel P, Dando O, Jiwaji Z, Baxter P, Todd AC, Heron S, et al. Neurons and neuronal activity control gene expression in astrocytes to regulate their development and metabolism. Nat Commun. 2017;8:15132.
32. Hartmann CA, Martins VR, Lima FR. High levels of cellular prion protein improve astrocyte development. FEBS Lett. 2013;587(2):238–44.
33. Prinz M, Montrasio F, Furukawa H, van der Haar ME, Schwarz P, Rulicke T, et al. Intrinsic resistance of oligodendrocytes to prion infection. J Neurosci. 2004;24(26):5974–81.
34. Diedrich JF, Bendheim PE, Kim YS, Carp RI, Haase AT. Scrapie-associated prion protein accumulates in astrocytes during scrapie infection. Proc Natl Acad Sci U S A. 1991;88(2):375–9.
35. Krejciova Z, Alibhai J, Zhao C, Krencik R, Rzechorzek NM, Ullian EM, et al. Human stem cell-derived astrocytes replicate human prions in a PRNP genotype-dependent manner. J Exp Med. 2017;214(12):3481–95.
36. Victoria GS, Arkhipenko A, Zhu S, Syan S, Zurzolo C. Astrocyte-to-neuron intercellular prion transfer is mediated by cell-cell contact. Sci Rep. 2016;6:20762.

SUPPORTING INFORMATION

Additional supporting information may be found in the online version of the article at the publisher's website.

Fig S1

FIGURE S1 (A) Polymerase chain reaction (PCR) performed on tail biopsies of seven transgenic founder mice revealed successful integration of CAT-PrP transgene. For control, we used CAT-PrP cDNA and DNA extracted from wild-type C57BL6/J mouse tail biopsies. Actin was

simultaneously amplified as a positive control. Samples were migrated on 2% agarose in Tris–EDTA buffer by electrophoresis. Lines 208, 214, and 215 failed to transmit the transgene to F1 generation. (B) Immunohistochemistry of brain sections of Syn^{Cre};loxPrP and $GFAP^{Cre}$;loxPrP mice with anti-PrP^{C} antibody POM2. Left panel: Whole brain section montage. Right panel: Magnified images of cerebellum and hippocampal regions stained with POM2. Images reveal differential PrP^{C} distribution in Syn^{Cre};loxPrP and $GFAP^{Cre}$;loxPrP mice

Fig S2

FIGURE S2 (A) Microglia (Iba1) and astrocyte (GFAP) immunostaining of the hippocampal sections of prion-inoculated Syn^{Cre};loxPrP (379 dpi), $GFAP^{Cre}$;loxPrP (627 days), loxPrP (504 dpi), and wild-type (184 dpi) mice. Expression of GFAP and Iba1 was upregulated in $Prnp^{+/+}$ mice, whereas Syn^{Cre};loxPrP and $GFAP^{Cre}$;loxPrP revealed significantly lower expression levels of the two markers. **(B)** Biological process enrichment obtained by gene ontology analysis on the upregulated genes in prion-infected $GFAP^{Cre}$;loxPrP mice revealed that most upregulated genes were involved in pathways associated with hormone response

Fig S3

FIGURE S3 Uncropped western blots. All western blots pertaining to this study are shown here in their original format as generated by the blot imager software. Sequence of staining in case multiple antibodies were used is indicated by numbering. No editing was performed

Table S1

TABLE S1 Table including detailed RNA Sequencing results including the differentially expressed genes, p-values, FDR values in prion-infected $GFAP^{Cre}$;loxPrP mice

Table S2

TABLE S2 Table showing differentially expressed genes that are common to prion disease (PrD) and prion-infected $GFAP^{Cre}$;loxPrP mice ($GFAP^{Cre}$;loxPrP prion)

How to cite this article: Lakkaraju AKK, Sorce S, Senatore A, Nuvolone M, Guo J, Schwarz P, et al. Glial activation in prion diseases is selectively triggered by neuronal PrP^{Sc}. Brain Pathol. 2022;00:e13056. https://doi.org/10.1111/bpa.13056